

STRUCTURAL-PHASE TRANSFORMATIONS OF AN FCC-ALLOY DURING THERMAL CYCLING

P. A. Chaplygin,² M. D. Starostenkov,² A. I. Potekaev,^{1,4}
A. A. Chaplygina,² A. A. Klopotov,^{4,5} V. V. Kulagina,^{3,4}
and L. S. Grinkevich¹

UDC 538.913

Using an intermetallic compound of the Ni–Al system as an example, it is shown by the Monte Carlo technique that the processes developed during thermal cycling in the course of structural phase transformations in FCC-alloys are irreversible. As a result of a heating–cooling cycle, a certain hysteresis is observed, whose presence suggests an irreversibility of these processes, which is indicative of the difference in the structural-phase states in the stages of heating and cooling. An analysis of the atomic and phase structure of the intermetallic system during its heating–cooling, i.e., in the course of order–disorder and disorder–order phase transformations has supported the difference in its structural-phase states in the stages of heating and cooling. Upon completion of the disorder–order phase transition, two antiphase domains with B2 superstructure are formed in the system. It is demonstrated that to ensure an order–disorder transition the system has to be somewhat overheated in contrast to a commonly acknowledged phase transformation temperature, while to achieve a disorder–order transition it has to be somewhat overcooled with respect to this temperature.

Keywords: order–disorder phase transition, simulations, structural-phase transformations, condensed matter systems.

INTRODUCTION

Currently the focus of attention is on the materials possessing a combination of special properties capable of maintaining them under extreme conditions. Ordering alloys and intermetallics, from this standpoint, offer a great practical promise due to a range of unique physical and physical-mechanical properties, such as high strength, thermal strength, magnetic properties, etc. These are primarily determined by the structural-phase state of a metallic system. Designing materials with a predetermined set of properties is far from being trivial. An investigation of the properties and structural-phase states of a material using experimental methods is laborious and costly. Moreover, it is frequently hard to reveal the mechanisms underlying the structural-phase transformations. We can alleviate these difficulties using computer simulations, since many of the processes and phenomena are difficult to observe in a physical experiment. For this reason, the systematic studies by the methods of computer simulation are of special attention and value, since they uncover the phenomena and physical-chemical processes taking place in the system [1–3]. To name but a few, for instance, a series of studies report investigations dealing with structural-phase states in an fcc-system using Cu–Au and Cu–Pt systems as an example [4–17]. It is for this reason that BCC-alloys, such as intermetallics of the Ni–Al system attract attention as the base materials with a set of unique properties for designing new refractory intermetallic alloys.

¹National Research Tomsk State University, Tomsk, Russia; ²I. I. Polzunov Altai State Technical University, Barnaul, Russia; ³Siberian State Medical University, Tomsk, Russia; ⁴V. D. Kuznetsov Siberian Physical-Technical Institute at Tomsk State University, Tomsk, Russia; ⁵Tomsk State Architecture and Building University, Tomsk, Russia, e-mail: genphys@mail.ru; kanc@spti.tsu.ru. Translated from *Izvestiya Vysshikh Uchebnykh Zavedenii, Fizika*, No. 4, pp. 52–57, April, 2015. Original article submitted September 29, 2014.

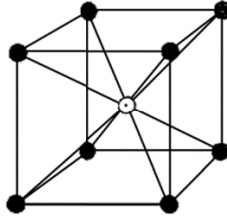


Fig. 1. Superstructure *B2*.

The purpose of this work is using numerical simulations (by the Monte Carlo method) to investigate the structural-phase characteristics of a BCC-alloy in the course of thermal cycling.

THE MODEL AND APPROXIMATIONS

In order to study the structural-phase transformations of a BCC-alloy under thermal cycling, let us use a NiAl alloy of an extensively modeled Ni–Al system.

It is well known that the atoms in the intermetallic nickel aluminide alloy are sitting in the nodes of the BCC-lattice in accordance with the *B2* superstructural ordering (Fig. 1).

Since we are concerned here with thermal cycling (increasing the system temperature followed by its decreasing), let us perform Monte Carlo simulations in a manner similar to our earlier investigations [4, 5, 9–15]. Let us assume a central pair interaction between atoms and prescribe interatomic interaction as a central Morse potential well suited for the problems of this kind [4, 5, 9–15]:

$$\varphi(r) = D \cdot \beta \cdot e^{-\alpha r} (\beta \cdot e^{-\alpha r} - 2),$$

where r is the spacing between the paired atoms and D , α , β are the parameters of the potential.

Let us reduce our considerations to the atomic interaction within the first three coordination spheres, and then the configurational energy of the system will be given by the following:

$$E = \frac{1}{2} \sum_{i=1}^N \sum_{j=1}^M \varphi(r_i - r_j),$$

where $r_i - r_j$ is the spacing between atoms i and j , N is the number of atoms in the crystal, and M is the number of neighbors in the three coordination spheres.

The computational grid represents a BCC-structure ordered in accordance with superstructure *B2* (NiAl alloy), the grid dimensions being $32 \times 32 \times 32$ cells (65536 atoms). Use is made of the periodic boundary conditions, which allowed us to prescribe an infinite crystal with the periodic structure in the form of the computational grid.

In order to activate the process of diffusion, one vacancy was introduced into the crystal, which corresponded to the concentration equal to $\sim 1.81 \cdot 10^{-5}$. Atomic diffusion followed the vacancy mechanism. The state of the alloy was changed within discrete periods of time; one act of self-diffusion was taken to be a single iteration, which corresponded to hopping of the atom into the respective node.

The short-range order parameter shall be determined using the Cowley approximation [18] and the long-range order parameter shall be determined within the Gorskii–Brag–Williams approximation [19]. To ensure thermal cycling, the alloy shall be heated in a stepwise manner from 200 to 2200 K, followed by a stepwise cooling to the initial temperature. The step of temperature variation was 100 K, with $5 \cdot 10^6$ iterations being made within every step.

TABLE 1. Parameters of the Morse Potential for the NiAl Alloy

Type of interaction	α	β	D
Ni–Ni	1.360166	37.72	0.451
Ni–Al	1.073363	17.551	0.6016
Al–Al	1.024939	27.743	0.3724

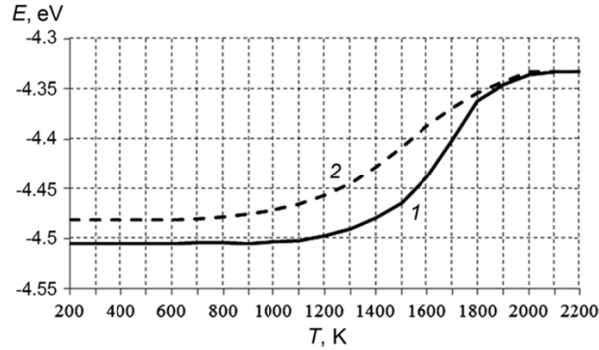


Fig. 2. Average configurational energy per atom during successive heating (Curve 1) and cooling (Curve 2).

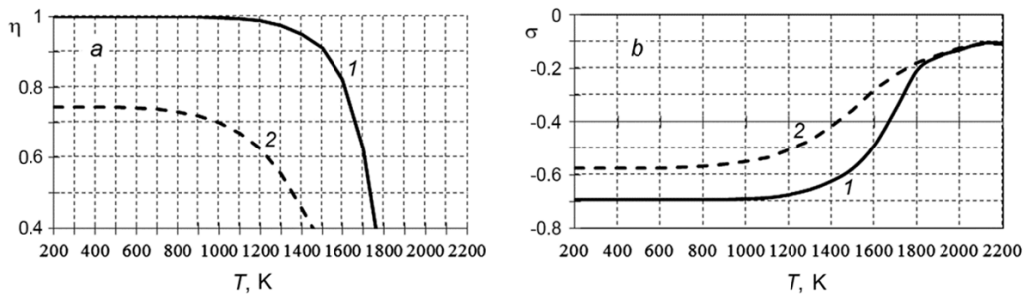


Fig. 3. Long-range (a) and short-range (b) order parameters in the course of consecutive heating (Curve 1) and cooling (Curve 2).

RESULTS AND DISCUSSION

The interatomic interaction was described using the Morse potential parameters presented in Table 1. The values of the potential were tabulated as the energy variation as a function of interatomic spacings.

Under cycling conditions, we investigated the average configurational energy per atom (Fig. 2) and the long-range (Fig. 3a) and short-range (Fig. 3b) order parameters.

It is clear from Fig. 2 that at the temperatures lower than 900 K the average configurational energy per atom does not undergo any variations during heating or cooling, its value however being appreciably higher during cooling. A gradual increase in the energy is observed within the range of temperatures from 1400 to 1900 K, which corresponds to the disordering processes (Fig. 3), implying that an order–disorder phase transition takes place in this interval. It is evident that the temperature interval of variation in the short-range and long-range order parameters (Fig. 3) is consistent with that of variations in the configurational energy (Fig. 2). As a result of the heating and cooling cycle there is a certain hysteresis (Fig. 2), whose presence under thermal cycling indicates an irreversibility of the processes and suggests different structural-phase states of the material in these stages of heating and cooling. This affects the

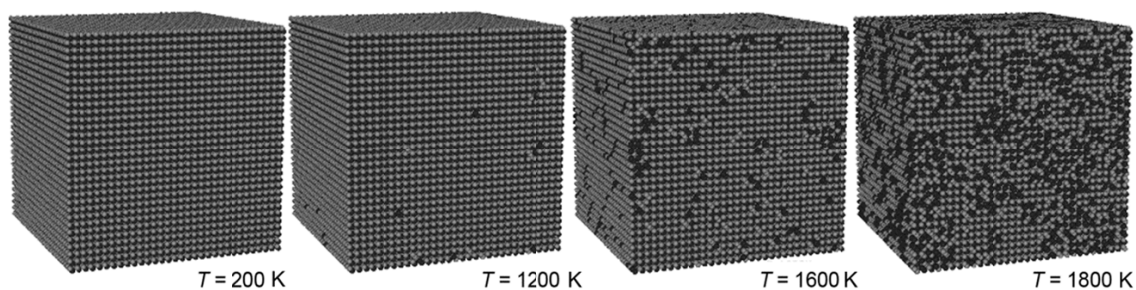


Fig. 4. Atomic structure of the alloy under study versus the temperature during stepwise heating.

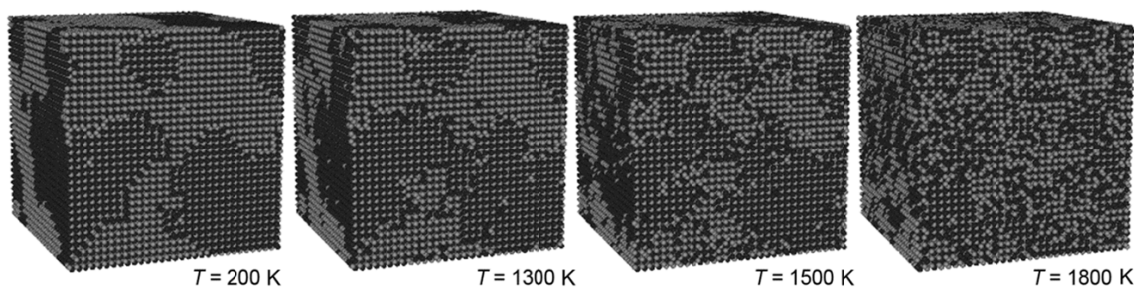


Fig. 5. Atomic structure of the alloy under study versus the temperature during stepwise cooling.

average characteristics of the system with increasing temperature, specifically, the long-range (Fig. 3a) and short-range (Fig. 3b) order parameters. One can readily see that the numerical values of these characteristics are significantly different at the same temperature in the heating and cooling stages. Thus, even the behavior of the average characteristics of the system evidences of irreversibility of the processes taking place in the course of the order–disorder phase transition under thermal cycling.

During heating, as demonstrated in Fig. 3, no distortions are observed in the long-range order in the course of the order – disorder phase transition up to the temperature 1200 K, and further up to 1600 K the value of the long-range order is gradually decreased. A sharp jump in the temperature curve of the long-range order plot occurs at $T = 1700$ K, which indicates a swift disordering in the system. With the temperature further increasing, the long-range order tends to zero, indicating disordering in the system.

Under cooling, there is no short-range ordering to the temperature $T = 1600$ K, it however appears at the temperatures below 1800 K (Fig.3b). A sharp increase in the long-range order parameter is observed within the range of temperatures 1100–1400 K, which suggests an order – disorder phase transition in this temperature interval. At the temperatures lower than 800 K, there are no variations in the long-range order parameter and the system is found in the ordered state.

Since a certain hysteresis is observed (Fig. 2) during the heating-cooling cycle, whose presence suggests irreversibility of the processes occurring in the material, we can assume differences in the structural-phase states in these stages of heating and cooling. To clarify this, let us analyze the atomic and phase structure of the system during heating-cooling, i.e., in the course of the order–disorder phase transition. Figures 4 and 5 present the atomic structure of the alloy under study as a function of the temperature of the order–disorder and disorder–order phase transitions, respectively.

In the course of heating (Fig. 4) up to the temperature 1000 K the alloy appears to be ordered; when the temperature is increased to $T = 1200$ K the first disordered regions are observed. As the temperature is further increased to 1600 K, the number and dimensions of the regions exhibiting distortion of the superstructural atomic arrangement is

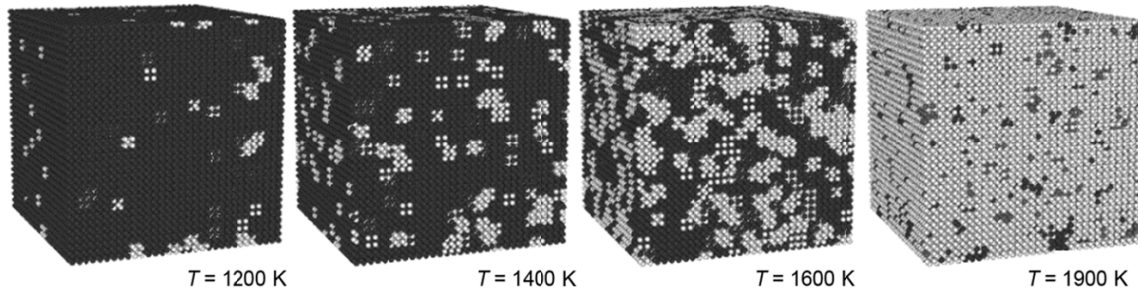


Fig. 6. Pattern of atomic distribution over the ordered and disordered phases in the NiAl alloy during heating.

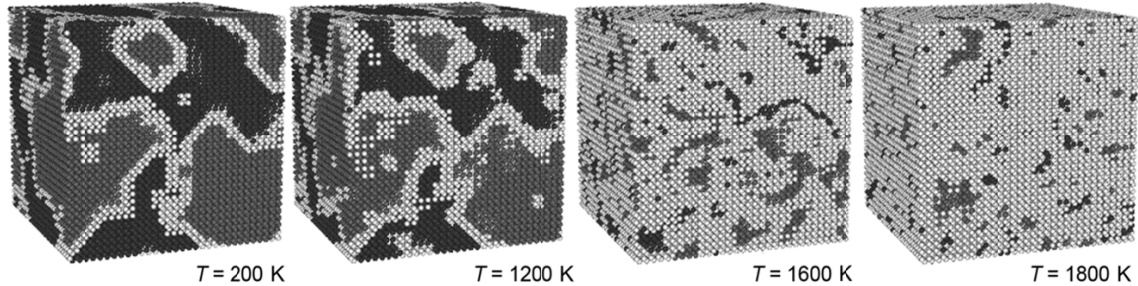


Fig. 7. Pattern of atomic distribution over the ordered and disordered phases in the NiAl alloy during cooling.

growing. When the temperature is as high as 1800 K, considerable distortions in the atomic order are observed, and at 1900 K the alloy is completely disordered.

When the system cools (Fig. 5) with the temperature decreasing to 1800 K, the regions ordered in accordance with superstructure *B2* appear. At $T = 1600$ K, the number and size of the ordered regions increase, and at the temperature lower than 1300 K the alloy is in the ordered state.

Comparing the atomic structure of the system during heating (Fig. 4) and cooling (Fig. 5), i.e., in the course of the order–disorder and disorder–order phase transitions, one can readily see the differences. During heating, the ordered regions persist up to higher temperatures than those observed under cooling when disordered regions begin to appear.

The structural-phase transitions during the order–disorder and disorder–order transitions represent a clear interest, particularly, in terms of the changes in the domain structure. Figures 6 and 7 illustrate the changes in the domain (phase) structure as a function of the temperature in the course of heating (Fig. 6) and cooling (Fig. 7).

In the course of heating up to $T = 1000$ K, the alloy is completely ordered, while within the temperature interval from 1100 to 1200 K the first disordered regions begin to appear. An increase in the temperature up to 1500 K gives rise to an increased number of disordered regions and at $T = 1600$ K they are uniformly distributed over the entire system. Upon further increase in the temperature up to 1800 K, practically the entire specimen is disordered, and at the temperature as high as 1900 K there are only nuclei of the domains left in the alloy.

In the cooling cycle down to the temperature 1800 K, only domain nuclei are observed in the material, with the size of antiphase domains with *B2* ordering being increased in the course of cooling to 1600 K. At lower (1300 K) temperature, no disordered regions are found in the alloy, except for the domain boundaries. It is worth mentioning that during further increase in the temperature the shape of the boundaries changes: the like type domains coalesce and persist up to 200 K. The difference in the values of configurational energy per atom upon completion of the heating–cooling cycle (Fig. 2) is due to the formation of two antiphase boundaries in the course of the disorder–order phase transition.

Comparing the phase distributions during heating (order–disorder transition, Fig. 6) and cooling (disorder–order transition, Fig. 7), we can draw a conclusion that the phase transition temperature during heating is higher than during cooling, which is consistent with the temperature plots for energy (see Fig. 2) and order (see Fig. 3). This implies

that in order to ensure an order–disorder transition the system has to be somewhat overheated with respect to the traditionally perceived phase transition temperature and, on the other hand, to ensure a disorder–order transition the alloy has to be somewhat overcooled with respect to this temperature. This is in agreement with the temperature dependences for energy and order. Upon completion of the disorder – order phase transition, two antiphase domains of superstructure *B2* are formed.

SUMMARY

Using Monte Carlo simulations, we have demonstrated that during cycling of BCC-alloys, such as for instance a NiAl intermetallic compound of the Ni–Al system, the processes observed are irreversible. as a result of the heating–cooling cycle, a certain hysteresis is formed in the temperature curve, whose presence is an evidence of irreversibility of the processes, which suggests differences in the structural phase states in the heating and cooling stages. An analysis of the atomic and phase structure in the course of the heating–cooling cycles, i.e., during the order–disorder and disorder–order phase transitions has supported the differences in the structural-phase states of the alloy. A comparison of the phase distributions during heating (order–disorder transition) and cooling (disorder–order transition) has allows us to conclude that during heating the phase transition temperature is higher than it is during cooling. This agrees with the temperature plots for energy and order. Upon completion of the disorder–order phase transition, two antiphase domains of superstructure *B2* are formed.

Thus, in order to ensure an order–disorder transition the system has to be somewhat overheated with respect to the conventionally accepted phase transition temperature and, on the other hand, to ensure a disorder–order transition the alloy has to be somewhat overcooled with respect to this temperature.

REFERENCES

1. M. D. Starostenkov, N. N. Medvedev, and O. V. Pozhidaeva, *Mater. Sci. Forum*, **567–568**, 165–168 (2008).
2. A. I. Potekaev, V. A. Starenchenko, V. V. Kulagina, *et al.*, *Low-Stability States of Metallic Systems* (Ed. A. I. Potekaev) [in Russian], Tomsk, NTL Publ. (2012).
3. A. I. Potekaev, M. D. Starostenkov, and V. V. Kulagina, *The Effect of Point and Planar Defects on Structural-Phase Transformations in a Pre-Transitional Low-Stability Region of Metallic Systems* (Systems (Ed. A. I. Potekaev) [in Russian], Tomsk, NTL Publ. (2014).
4. A. I. Potekaev, E. A. Dudnik, M. D. Starostenkov, *et al.*, *Russ. Phys. J.*, **53**, No. 3, 213–224 (2010).
5. A. I. Potekaev, E. A. Dudnik, M. D. Starostenkov, V. V. Kulagina, *et al.*, *Russ. Phys. J.*, **53**, No. 5, 465–479 (2010).
6. A. I. Potekaev and V. V. Kulagina, *Russ. Phys. J.*, **54**, No. 8, 839–854 (2011).
7. A. I. Potekaev and V. V. Kulagina, *Izv. Vyssh. Uchebn. Zaved. Fiz.*, **52**, No. 8/2, 456–459 (2009).
8. A. A. Klopotov, A. I. Potekaev, É. V. Kozlov, and V. V. Kulagina, *Russ. Phys. J.*, **54**, No. 9, 1012–1023 (2012).
9. A. I. Potekaev, A. A. Chaplygina, M. D. Starostenkov, *et al.*, *Fund. Probl. Sovr. Materialoved.*, **54**, No. 4, 117–124 (2011).
10. A. I. Potekaev, A. A. Chaplygina, M. D. Starostenkov, *et al.*, *Fund. Probl. Sovr. Materialoved.*, **9**, No. 3, 367–374 (2012).
11. V. V. Kulagina, A. A. Chaplygina, A. A. Popova, *et al.*, *Russ. Phys. J.*, **55**, No. 7, 814–824 (2012).
12. A. I. Potekaev, S. V. Dmitriev, V. V. Kulagina, *et al.*, *Low-Stability Long-Period Structures in Metallic Systems* [in Russian], Tomsk, NTL Publ. (2010).
13. A. I. Potekaev, A. A. Chaplygina, M. D. Starostenkov, *et al.*, *Fund. Probl. Sovr. Materialoved.*, **9**, No. 4, 503–509 (2012).
14. A. I. Potekaev, V. V. Kulagina, A. A. Chaplygina, *et al.*, **55**, No. 11, 1248–1257 (2013).
15. A. I. Potekaev, V. V. Kulagina, A. A. Chaplygina, *et al.*, **56**, No. 6, 620–629 (2013).

16. V. V. Kulagina, A. I. Potekaev, A. A. Klopotov, and M. D. Starostenkov, *Russ. Phys. J.*, **55**, No. 4, 323–361 (2012).
17. A. I. Potekaev, A. A. Klopotov, V. E. Gunther, and V. V. Kulagina, *Izv. Vyssh. Uchebn. Zaved. Chern. Metallurg.*, No. 10, 61–67 (2010).
18. V. I. Iveronova and A. A. Kantselson, *Short-Range Order in Solid Solutions* [in Russian], Moscow, Nauka (1977).
19. M. A. Krivoglaz and A. A. Smirnov, *The Theory of Ordering Alloys* [in Russian], Moscow, Fizmatgiz (1958).